FULL PAPER

Dalton
www.rsc.org/dalton

Molecular structure of trimethylphosphine–gallane, $Me_3P{\cdot}GaH_3$: gas-phase electron diffraction, single-crystal X-ray diffraction, and quantum chemical studies †

Christina Y. Tang,[a] Robert A. Coxall,[b] Anthony J. Downs,*[a] Tim M. Greene,[c] Lorna Kettle,[b] Simon Parsons,[b] David W. H. Rankin,[b] Heather E. Robertson[b] and Andrew R. Turner[b]

[a] *Inorganic Chemistry Laboratory, University of Oxford, South Parks Road, Oxford, UK OX1 3QR*

[b] *School of Chemistry, University of Edinburgh, West Mains Road, Edinburgh, UK EH9 3JJ*

[c] *School of Chemistry, University of Exeter, Stocker Road, Exeter, UK EX4 4QD*

Received 12th June 2003, Accepted 31st July 2003
First published as an Advance Article on the web 15th August 2003

The structure of the gallane adduct $Me_3P{\cdot}GaH_3$ in the vapour and crystalline states has been investigated. The gas-phase electron-diffraction (GED) pattern has been analysed using the SARACEN method to determine the most reliable structure of the gaseous molecule. Salient structural parameters (r_{h1} structure) were found to be: *r*(Ga–H) 159.0(11), *r*(Ga–P) 244.3(6), *r*(P–C) 184.0(2), *r*(C–H) 108.3(7) pm; H–Ga–P 98.4(12) and Ga–P–C 117.7(3)°. The structure of a single crystal at 150 K shows that the adduct retains the same monomeric unit in the crystalline phase, with dimensions generally close to those of the gaseous molecule and an eclipsed conformation of the C_3PGaH_3 skeleton. The results are discussed and analysed in the light of quantum chemical calculations and of the properties of related adducts of Group 13 metal hydrides.

Stabilisation of the binary metal hydride by coordination to a nitrogen, phosphorus or oxygen base is a familiar feature of Group 13 chemistry.[1–6] Accordingly, adducts such as $Me_3N{\cdot}GaH_3$ and $Me_3P{\cdot}GaH_3$ are source materials altogether more convenient than gallane itself for reactions that exploit the facility of gallium-bound hydrogen ligands to act as leaving groups in decomposition, metathesis, reduction or elimination processes. Numerous experimental studies testify to the influence of the electronic properties, geometry and bulk of the base on the structure and stability of the resulting complexes. In addition, the structural, vibrational and thermodynamic properties of species like $H_3E{\cdot}GaH_3$ (E = N, P or As)[7] and $H_2O{\cdot}GaH_3$[8] have attracted quantum chemical analysis.

Despite the early report, based on the displacement reaction in benzene solution,[9] that trimethylamine and trimethylphosphine have similar donor strengths with respect to gallane, phosphine complexes of the type $R_3P{\cdot}GaH_3$ have differed from their amine counterparts in finding only limited applications as gallane sources.[3–5] What is perhaps most noteworthy, however, is how much more effectively a phosphine binds to GaH_3 than to AlH_3, whereas the reverse order is found with an amine. Indeed the Al⟵P interaction is sufficiently weak that adducts containing sterically non-hindered phosphines decompose to polymeric $[AlH_3]_n$ under relatively mild conditions.[10]

Here we report the results of experimental and theoretical studies on one of the simplest and best known phosphine complexes of gallane, *viz*. $Me_3P{\cdot}GaH_3$. Prepared in effect by the reaction of $LiGaH_4$ with $[Me_3PH]Cl$ in diethyl ether solution, this was first reported in 1965[9] as a white solid which can be sublimed *in vacuo* at ambient temperatures. The compound has been characterised by its vibrational[9,11] and NMR[9] spectra, but no structural details have been reported previously. Although the crystal structures of the complexes $Bu^t_3P{\cdot}GaH_3$,[12a] $Cy_3P{\cdot}GaH_3$,[12b] and $H_3Ga{\cdot}Me_2PC_2H_4PMe_2{\cdot}GaH_3$[12b] have been described, there is insufficient evidence to establish any clear pattern that reflects on the bonding of such complexes. More particularly, no attempt has been made hitherto, so far as we are aware, to determine the structure of a *gaseous* phosphine–gallane complex. Even in the case of $Me_3N{\cdot}GaH_3$, which suffers no radical change of structure, there is a 5.3(6) pm elongation of the Ga–N bond on vaporisation of the crystal, suggesting a reduced degree of N⟶Ga charge transfer in the gaseous molecule.[13]

Accordingly, we have set out to determine not only the crystal structure of $Me_3P{\cdot}GaH_3$ at 150 K by X-ray diffraction, but also the structure of the gaseous molecule by gas electron diffraction (GED). The complex is somewhat less volatile than its trimethylamine analogue, for which a similar study has been described,[13] and GED studies have been severely hampered by the combination of this factor with the relatively low thermal stability and reactivity of the $Me_3P{\cdot}GaH_3$ molecule. Thus, there is only a narrow temperature range (< 20 °) over which the flux of vapour can be maintained at a level just sufficient to give useful scattering. Attempts to increase the flux by raising the temperature above *ca*. 40 °C result only in decomposition to give significant proportions of the free phosphine and (highly labile) gallane.[2,14] Even with the benefit of a satisfactory scattering pattern for the molecule, there are limits to the structural details that can be established well by electron diffraction alone. A major improvement in the reliability and quality of the structural refinement of such a molecule is now possible, however, with the advent of the SARACEN method.[15] The essential feature of SARACEN is that information calculated *ab initio* is introduced into the refinement procedure as additional observations (or restraints), the weight of the observation being assigned according to the level of convergence achieved in a series of graded *ab initio* calculations. Hence it has been possible, for example, to refine simultaneously the values of all the structural parameters and all significant amplitudes of vibration for the gallane molecules $Me_3N{\cdot}GaH_3$,[13] $H_2GaB_3H_8$,[16] and H_2GaBH_4.[17] The structure of the gaseous $Me_3P{\cdot}GaH_3$ molecule determined in this way is then compared with the structure in the crystal at 150 K. The results of experiment and theory are reviewed for whatever light they shed on the structure and stability of this and related complexes of alane and gallane.

† Electronic supplementary information (ESI) available: Cartesian coordinates and least squares correlation matrix for $Me_3P{\cdot}GaH_3$. See http://www.rsc.org/suppdata/dt/b3/b306736j/

DOI: 10.1039/b306736j

Table 1 Nozzle-to-plate distances, weighting functions, correlation parameters, scale factors and electron wavelength for the GED study of trimethylphosphine–gallane, $Me_3P{\cdot}GaH_3$

Nozzle-to-plate distance/mm	Weighting functions/nm^{-1}					Correlation parameter (p/h)	Scale factor, k[a]	Electron wavelength[b]/pm
	Δs	s_{min}	sw_1	sw_2	s_{max}			
127.62	40	100	120	264	308	0.436	1.605(98)	6.016
285.21	20	40	60	110	128	0.473	1.095(46)	6.016

[a] Figures in parentheses are estimated standard deviations of the last digits. [b] Determined by reference to the scattering pattern of benzene vapour.

Table 2 Calculated optimised molecular geometry for $Me_3P{\cdot}GaH_3$ using *ab initio* methods and various basis sets (basis set/method, distances in pm and angles in °)

Parameter	6-31G(d)/RHF	6-31G(d)/MP2	6-311G(d,p)/MP2	6-311+G(d,p)/MP2	6-311G(df,p)/MP2	6-311+G(df,p)/MP2
r(Ga–P)	248.66	245.21	250.03	250.20	248.62	248.77
r(Ga–H)	158.99	159.88	159.06	159.09	159.50	159.50
r(P–C)	183.29	182.97	182.70	182.69	182.21	182.20
<H–Ga–P	99.7285	99.9734	98.7950	98.7911	99.0383	98.9852
<Ga–P–C	114.1050	114.2853	114.8557	114.9354	114.6928	113.7611
<C–P–C	104.4657	104.2570	103.5906	103.4988	103.7817	103.7016

Experimental

(a) Synthesis, crystal growth and manipulation of $Me_3P{\cdot}GaH_3$

Trimethylphosphine–gallane, $Me_3P{\cdot}GaH_3$, was prepared as described previously[9] by the reaction of freshly prepared $LiGaH_4$ with 1 mol equivalent each of Me_3P and HCl (both ex Aldrich) in dry Et_2O solution at room temperature. It was purified by fractional condensation *in vacuo* using a train of all-glass traps which had been pre-conditioned by 'flaming-out'.[2,14] The purified product collected in a trap held at −45 °C, its identity and purity being confirmed by reference to the IR spectrum of an annealed solid film at 77 K[11] and to the ^{1}H NMR spectrum[9,18] of a [$^2H_8$]toluene solution of the compound. The sample was then condensed in a pre-conditioned Pyrex glass ampoule which was kept at 0 °C. After three weeks colourless block crystals were observed to have formed on the walls of the vessel. A crystal suitable for study by X-ray diffraction was selected from under cold perfluoropolyether RS3000 oil.

(b) GED measurements

Electron-scattering patterns were recorded photographically on Kodak Electron Image films using the Edinburgh gas diffraction apparatus.[19] To counter the problems of thermal frailty and low vapour pressure at room temperature, the vapour over the crystalline solid at room temperature was expanded into a bulb of 2 dm^3 capacity. Thence the vapour was injected into the diffraction chamber *via* a metal nozzle held at room temperature with camera distances of *ca*. 128 and 285 mm. The accelerating voltage approximated to 40 kV, giving an electron wavelength near 6.0 pm. The precise camera distances and electron wavelengths were determined from scattering patterns for benzene vapour recorded immediately before or after the sample patterns. Details are given in Table 1, together with the weighting functions used to set up the diagonal terms of the band weight matrices, the s ranges, scale factors, and correlation parameters used to calculate the immediate off-diagonal terms of the band weight matrices.

Each exposed film was left under pumping for 24 h before removal, washed, and left in the air for 24 h before being developed. These steps minimised, but did not eliminate, the effects of fogging caused by the action of the strongly reducing vapour on the photographic emulsion. Details of the electron-scattering patterns were converted into digital form using a PDS densitometer at the Institute of Astronomy in Cambridge with a scanning program described elsewhere.[20] The data spanning the ranges $40 \le s \le 128$ and $100 \le s \le 308$ nm^{-1} were reduced and analysed by standard programs,[21] drawing on the scattering factors listed by Ross *et al.*[22]

(c) X-Ray diffraction measurements

Crystal data. $C_3H_{12}GaP$, M = 148.82, monoclinic, space group $P2_1/m$, a = 588.48(15), b = 921.2(2), c = 707.81(18) pm, β = 113.879(4)°, $V = 350.9 \times 10^6$ pm^3, λ = 71.073 pm, Z = 2, D_c = 1.409 Mg m^{-3}, $F(000)$ = 152.509, T = 150 K, colourless block 0.07 × 0.07 × 0.15 mm, μ(Mo-Kα) = 4.020 mm^{-1}.

Data were collected using ϕ–ω scans on a Bruker Smart APEX diffractometer with graphite-monochromated Mo-Kα radiation. Of the 1874 reflections measured ($3 \le \theta \le 29°$; $-7 \le h \le 7$, $0 \le k \le 12$, $0 \le l \le 9$) 918 were unique (R_{int} 0.02). An absorption correction was applied using the multi-scan procedure SADABS[23] (T_{min} = 0.765, T_{max} = 1).

The crystal structure was solved by direct methods (SHELXS).[24] Hydrogen atoms were located in a difference map and refined subject to similarity restraints on the Ga–H and C–H bond distances; common isotropic displacement parameters were refined for hydrogens attached to the same atom. All non-hydrogen atoms were modelled with anisotropic displacement parameters. The refinements then proceeded by full-matrix least squares against F^2 (CRYSTALS)[25] to give a final conventional R of 0.0226 [based on F and 845 data with $F > 4\sigma(F)$] and wR_2 = 0.0575 (based on F^2 and all 918 data). The final difference map extrema were +0.74 and −0.33 e Å^{-3}.

CCDC reference number 212672.

See http://www.rsc.org/suppdata/dt/b3/b306736j/ for crystallographic data in CIF or other electronic format.

(d) Theoretical calculations

Both *ab initio* and density functional theory (DFT) calculations were carried out with the Gaussian 98 program suite.[26] Details of the calculated energies of the minima found for the $Me_3P{\cdot}GaH_3$ molecule using three different methods are given in Tables 2 and 3. We have performed restricted Hartree–Fock (RHF) calculations; electron correlation was then included using a second-order Møller–Plesset perturbation expansion (MP2); and we have also performed density functional theory (DFT) calculations with the standard B3PW91 hybrid functional.[27]

Geometry optimisations at the RHF and MP2 levels were undertaken using both double-ζ (6-31G) and triple-ζ [6-311G(d,p)] basis sets.[28–30] The effects of adding diffuse and polarisation functions were also investigated by performing calculations at the MP2 level using the 6-311+G(d,p),

Table 3 Calculated optimised molecular geometry for $Me_3P{\cdot}GaH_3$ using the DFT-B3PW91 method and various basis sets (distances in pm, angles in °)

	Basis set		
Parameter	6-31G(d)	6-31G(d,p)	6-311G(d,p)
r(Ga–P)	240.27	240.36	246.31
r(Ga–H)	157.69	158.40	157.88
r(P–C)	183.48	183.27	183.20
<H–Ga–P	100.3135	100.2333	99.5167
<Ga–P–C	114.0240	113.9080	114.4661
<C–P–C	104.5593	104.6928	104.0467

6-311G(df,p) and 6-311+G(df,p) basis sets.[30,31] It was important to include the Ga 3d orbitals in the electron correlation scheme since the estimated orbital energies show that the Ga 3d electrons lie closer in energy to the 4s and 4p valence orbitals than to the remaining inner core orbitals.[16,17] Therefore the frozen core approximation was employed for all MP2 calculations, with the core defined as the 1s–3p orbitals. Highest level estimates of the energy and geometric parameters were gained from MP2 calculations with a 6-311+G(df,p) basis set.

DFT calculations were carried out with 6-31G, 6-31G(d,p) and 6-311G(d,p) basis sets.[27–30] The effects of adding further polarisation functions were investigated with calculations involving a 6-311G(df,p) basis set.[30,31]

Dissociation energies have been calculated for the following alane and gallane adducts: $H_3N{\cdot}AlH_3$, $H_3N{\cdot}GaH_3$, $Me_3N{\cdot}AlH_3$, $Me_3N{\cdot}GaH_3$, $H_3P{\cdot}AlH_3$, $H_3P{\cdot}GaH_3$, $Me_3P{\cdot}AlH_3$ and $Me_3P{\cdot}GaH_3$. A 6-311++G(d,p) basis set was used for MP2 calculations on all relevant donors and acceptors and the adducts they form. The dissociation energies have been modified using the counterpoise correction to take some account of basis set superposition error.[32]

The vibrational force field associated with the optimised structure of $Me_3P{\cdot}GaH_3$ and described by Cartesian force constants (calculated using a 6-31G(d) basis set at the MP2 level) was transformed into one described by a set of symmetry coordinates using the program ASYM40,[33] and this served as the starting point for computing the vibrational properties of the molecule. The computed harmonic force field has also been scaled to match the experimental one reported by Odom *et al.*,[11] but this did not make any significant difference to the outcome of the GED refinement calculations. The results reported here relate to the unscaled force field. On this basis, vibrational amplitudes, *u*, have been estimated, together with perpendicular amplitude corrections, *K*, for use in the analysis of the GED pattern.

Results

(a) Introduction and theoretical calculations

Precedent[3–5] gives us no reason to expect anything other than a discrete molecular structure for trimethylphosphine–gallane, with a tetra-coordinated Ga atom in both the vapour and solid phases. That is certainly the conclusion to be drawn from the vibrational spectra of the compound,[11] from the crystal structures of other phosphine–gallane complexes characterised to date,[12] and also from structural studies of $Me_3N{\cdot}GaH_3$ spanning the vapour as well as the solid state.[13] By contrast, the alane $Me_3N{\cdot}AlH_3$ is monomeric in the vapour[34] but dimeric in the crystal.[35] The present study is mainly concerned therefore with determining a reliable structure for the $Me_3P{\cdot}GaH_3$ molecule (including the GaH_3 fragment) and with establishing how it varies from one phase to another. In addition, we seek through quantum chemical calculations to compare the strength of the Ga⟵P with that of other coordinative interactions in order to gain a clearer insight into the factors determining the relative stabilities of such complexes.

A graded series of *ab initio* and DFT calculations was performed on $Me_3P{\cdot}GaH_3$ to determine the effects of changes in the theoretical method and basis set on the computed molecular geometry, with the results presented in Tables 2 and 3. As expected, the equilibrium geometry is found invariably to have a staggered C_3PGaH_3 skeleton conforming to C_{3v} symmetry. The Ga–P bond distance was found to be the parameter most sensitive to the choice of basis set. When electron correlation was included, this distance varied between 245.2 and 250.2 pm, with larger basis sets leading to larger values, and increasing the number of polarisation functions leading to smaller ones. By contrast, the Ga–H distance is less sensitive to such changes, an increase in the number of polarisation functions giving a variation of only 1 pm. At the MP2 level, the Ga–H distance decreased by an insignificant 0.8 pm on improving the basis set from 6-31G to 6-311G(d,p), and subsequently lengthened by 0.5 pm when additional polarisation functions were introduced. The addition of diffuse functions is noted to have very little effect on the P–C bond length and on the angles H–Ga–P, Ga–P–C and H–C–H, with variations never exceeding 1 pm or 1°, respectively. The dimensions calculated for the molecule using the DFT-B3PW91 method are in good agreement with those at the MP2 level and show similar variations as a function of basis set.

(b) Gas electron diffraction (GED) measurements and analysis

Earlier studies have repeatedly emphasised the technical problems of carrying out gas electron diffraction (GED) measurements on such labile molecules as digallane[14] and its derivatives.[13,16,17] Numerous attempts were made to record satisfactory and reproducible scattering patterns for trimethylphosphine–gallane, particularly at the short camera distance (*ca.* 128 mm) before it was possible to secure an acceptable data set extending to a maximum value of 308 nm^{-1} in the variable s ($= 4\pi\lambda^{-1} \sin\theta$, where 2θ is the scattering angle).

The radial distribution curve, $P(r)/r$ *vs.* r, derived from the experiments after scaling, combination and Fourier transformation, is depicted in Fig. 1. In essence it comprises four main peaks centred near 110, 170, 250 and 380 pm. These correspond in order to scattering from (i) the bonded C–H atom pairs, (ii) the bonded Ga–H and P–C atom pairs, (iii) the bonded Ga–P atom pair, and (iv) the non-bonded Ga ⋯ C atom pairs, although P ⋯ H and Ga ⋯ H non-bonded atom pairs also make some contribution to the third and fourth peaks, respectively. The only other clearly discernible feature is a weak peak near 280 pm attributable to scattering from the C ⋯ C non-bonded atom pairs. The absence of any appreciable scattering at long range (r > 400 pm) is consistent with the

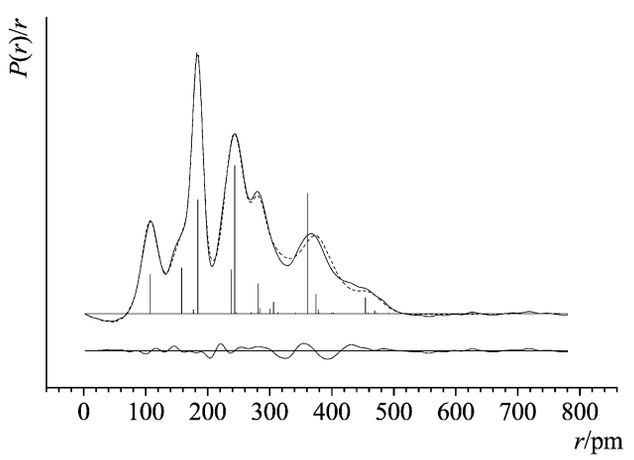

Fig. 1 Observed and final difference radial distribution curves for $Me_3P{\cdot}GaH_3$. Before Fourier inversion the data were multiplied by $s[\exp(-0.000\,02s^2)/(Z_{Ga} - f_{Ga})(Z_P - f_P)]$. Solid line: experimental curve; dashed line: theoretical curve.

presumption that the simple $Me_3P{\cdot}GaH_3$ molecule is the predominant vapour species.

In the light of the vibrational spectra[11] and the results of the quantum chemical calculations, we have adopted the structural model for the $Me_3P{\cdot}GaH_3$ molecule illustrated in Fig. 2 for electron diffraction refinements.[36] The GaH_3 and PC_3 units, each assumed to be regular pyramids, are linked together so that their local C_3 axes are coincident with the Ga–P bond; likewise the CH_3 groups are also taken to be regular pyramids, each with its C_3 axis coincident with the relevant P–C bond. Such a model requires for its specification nine independent geometric parameters. With reference to Fig. 2, these are the four interatomic distances Ga–P, P–C, Ga–H, and C–H (p_1–p_4), and angles Ga–P–C (p_5), H–Ga–P (p_6), H–C–H (p_7), α defining the twisting of the CH_3 groups away from the staggered conformation with respect to the $GaPC_2$ moiety (p_8), and β defining the twisting of the GaH_3 fragment away from the staggered H_3GaPC_3 conformation (p_9).

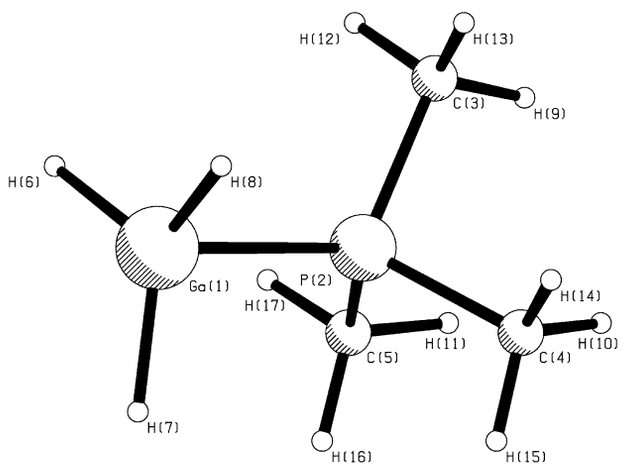

Fig. 2 View of the $Me_3P{\cdot}GaH_3$ molecule in the optimum refinement of the electron-diffraction data.

As in the case of the analogous trimethylamine adduct $Me_3N{\cdot}GaH_3$,[13] it was not possible to determine more than a rather basic structure for $Me_3P{\cdot}GaH_3$ on the basis of its electron diffraction pattern alone. Two features in particular militate against the precise positioning of the hydrogen atoms: (i) the distances P–C and Ga–H are quite similar and the parameters defining them are correspondingly correlated; and (ii) the hydrogen atoms contribute relatively little to the molecular scattering which is dominated by the heavy atoms. As a result several parameters could not be refined satisfactorily, namely the Ga–H distance, the angles Ga–P–C, H–Ga–P and H–C–H, and the vibrational amplitudes of the following units: Ga–P, Ga ··· H(13), P(2) ··· H(6) and C(4) ··· H(9). The results of the MP2 calculations with a 6-311+G(df,p) basis set have therefore been applied as flexible restraints on these parameters, and the SARACEN method[15] has then been adopted to allow the free refinement of all nine of the geometric parameters and most of the vibrational amplitudes. The remaining unrefined amplitudes [for P(2) ··· H(9), C(5) ··· H(12), C(5) ··· H(9), C(4) ··· H(13) and Ga(1) ··· H(12)] were then assigned values equal or linked to the refined amplitudes of related vectors. The torsional angles α and β could not be refined satisfactorily and each has therefore been fixed at 0.0° in accordance with the optimum geometry calculated for the molecule. In addition, we have constructed a harmonic force field using an MP2 calculation with a 6-311+G(df,p) basis set. This was then modified using the SHRINK program[37] in which vibrational motions are described by coordinates approximating more closely to true curvilinear pathways. Hence we have sought to gain more realistic estimates of vibrational correction terms (equivalent to K values) and so allow better for

Table 4 Geometric and vibrational parameters deduced by analysis of the electron diffraction pattern of gaseous $Me_3P{\cdot}GaH_3$[a]

(a)

	Geometric parameter	Value	Restraint
p_1	Ga–P	244.3(6)	
p_2	P–C	184.0(2)	
p_3	Ga–H	159.0(11)	159.5(10)
p_4	C–H	108.3(7)	109.0(10)
p_5	<GaPC	117.7(3)	114.8(10)
p_6	<HGaP	98.4(12)	99.0(10)
p_7	<HCH	111.1(11)	108.2(10)
p_8	α, CH_3 twist	0.0	(fixed)
p_9	β, GaH_3 twist	0.0	(fixed)

(b)

	Amplitude	Distance	Value	Restraint/constraint
u_1	P(2)–Ga(1)	243.7(6)	12.3(3)	8.0(8)
u_2	C(3) ··· Ga(1)	360.4(7)	44.7(50)	
u_3	C(3)–P(2)	183.9(2)	4.3(4)	
u_4	H(6)–Ga(1)	157.8(11)	12.4(20)	
u_5	H(9) ··· P(2)	237.8(16)	17.9	Tied to u_1
u_6	H(9)–C(3)	107.4(7)	8.7(8)	
u_7	C(4) ··· C(3)	281.4(7)	8.1(7)	
u_8	H(13) ··· Ga(1)	374.5(18)	30.7(33)	30.1(30)
u_9	H(12) ··· Ga(1)	374.5(18)	30.7	Tied to u_8
u_{10}	H(9) ··· Ga(1)	454.3(11)	18.5(41)	
u_{11}	H(6) ··· P(2)	306.3(27)	21.7(22)	20.3(20)
u_{12}	H(9) ··· C(4)	283.9(20)	18.9(23)	20.1(20)
u_{13}	H(12) ··· C(5)	300.2(16)	22.3	Tied to u_{11}
u_{14}	H(9) ··· C(5)	283.9(20)	18.9	Tied to u_{12}
u_{15}	H(13) ··· C(4)	300.9(16)	22.3	Tied to u_{11}

[a] For definitions of the parameters and details of the refinements see the text, and for atom numbering see Fig. 2. Distances and vibrational amplitudes, u, in pm; angles in °. Estimated standard deviations (e.s.d.s) are given in parentheses in units of the last digit. (a) SARACEN refinement with SHRINK analysis, r_{h1} structure.[37] (b) All amplitude distances are for the corresponding r_a structure.

'shrinkage' effects. The refinement affords the results listed in Table 4. Additional tables documenting the refinement (Cartesian coordinates and correlation matrix) are available in the Supplementary Information.† The quality of fit to the observed GED pattern may be judged by the final difference plots in Fig. 1 and 3 for the radial distribution and molecular-scattering curves. The final R factors (R_G) of 0.126, 0.180, and 0.148 for the short, long and combined data sets, respectively, are admittedly rather high, but not very different in fact from those characterising similar analyses of other gallium hydrides, *e.g.* Ga_2H_6[14] and $GaBH_6$.[17] As in earlier cases, the level of agreement between observed and computed data sets is necessarily compromised by impurities and fogging and the relatively poor signal-to-noise ratio of the measured scattering.

(c) X-Ray study of a single crystal

The X-ray diffraction study of a single crystal of $Me_3P{\cdot}GaH_3$ at 150 K confirms that the compound forms molecular crystals consisting of more or less discrete monomeric molecules. Selected distances and angles are included in Table 5. The shortest Ga ··· H and Ga ··· P contacts between different molecules are 336(2) and 469.3(1) pm, respectively, giving no hint of significant intermolecular interactions analogous to those responsible for the dimeric aggregates $[Me_3N{\cdot}AlH_3]_2$[35] and $[Me_2(H)N{\cdot}AlH_3]_2$[38] found in crystals of some amine complexes of alane and gallane. Fig. 4 shows the crystal packing of the solid.

Structural comparisons with the gaseous $Me_3P{\cdot}GaH_3$ molecule are complicated by differences of temperature and technique, with X-ray diffraction, unlike electron diffraction, measuring distances between centres of maximum electron

Table 5 Comparison of the geometric parameters of the $Me_3P{\cdot}GaH_3$ molecule derived (a) from the SARACEN + SHRINK analysis of the electron diffraction pattern of the vapour, (b) from *ab initio* calculations, and (c) from the structure of a single crystal at 150 K as determined by X-ray diffraction[a]

Parameter	Gaseous molecule GED, r_{h1}[b]	*Ab initio* calculations, r_e (MP2)[c]	Single crystal at 150 K, r_a
Bond distances			
Ga–P	244.3(6)	248.8	238.57(6)
P–C	184.0(2)	182.2	179.5(1)[d]
Ga–H	159.0(11)	159.5	154(1)[d]
C–H	108.3(7)	109.4	0.916(9)
Angles			
GaPC	117.7(3)	113.8	113.7(8)[d]
HGaP	98.4(12)	99.0	106.1(6)[d]
HCH	111.1(11)	108.2	109(3)
CH_3 twist, α	0.0[e]	0.0	0.0(4)[d]
GaH_3 twist, β	0.0[e]	0.0	58.8(2)[d]

[a] For definitions of the parameters see the text. Distances in pm, angles in °. Estimated standard deviations (e.s.d.s) are given in parentheses in units of the last digit. [b] See the text and Table 4. [c] Calculated using a 6-311+G(df,p) basis set. [d] Average value; sample standard deviation quoted. [e] Fixed at the *ab initio* value.

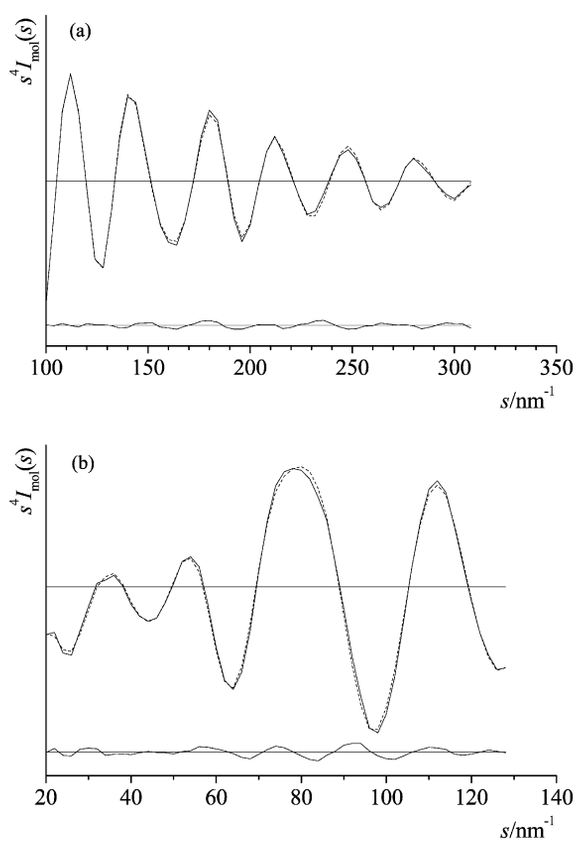

Fig. 3 Observed and final difference molecular-scattering curves for $Me_3P{\cdot}GaH_3$ with nozzle-to-plate distances of (a) 127.62 and (b) 285.21 mm. Solid lines: experimental molecular scattering intensities; dashed lines: theoretical molecular scattering intensities.

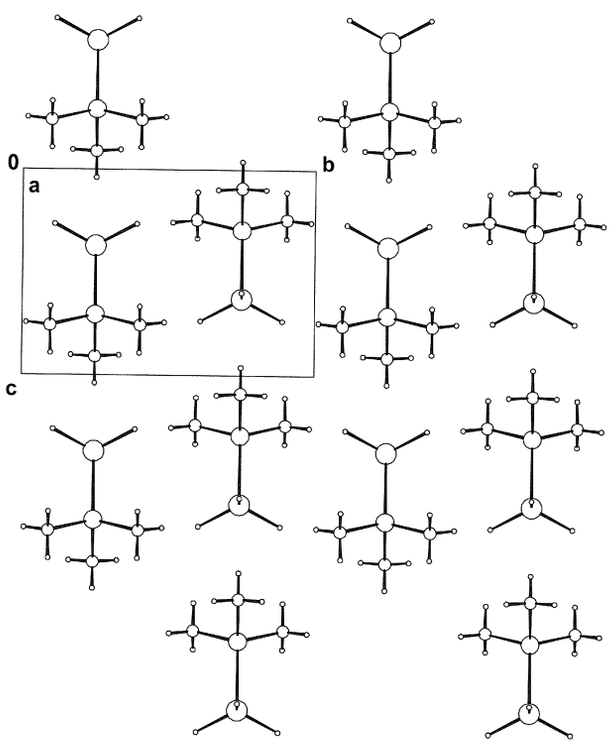

Fig. 4 Structure of solid $Me_3P{\cdot}GaH_3$ at 150 K.

density. In general, though, crystallisation affects the structure only in the following relatively subtle ways.

(i) It is noteworthy firstly that the molecule opts for an *eclipsed* rather than a staggered conformation of the C_3PGaH_3 skeleton and so appears to differ from the gaseous molecule. As a result of this finding, we repeated the refinement of the GED data with the molecule fixed in the eclipsed conformation to discover that this gives virtually identical results for the other main structural parameters. Furthermore, calculations reveal a stabilisation of the staggered over the eclipsed conformer amounting to only 3.4 kJ mol^{-1}. The results overall suggest that the GaH_3 unit is more or less freely rotating in the gas phase. The adoption of the eclipsed conformation by the molecule in the solid does contrast, however, not only with other phosphine–gallanes whose crystal structures have been determined,[12] but also with trimethylamine–gallane which favours a staggered geometry in both the vapour and the solid phases.[13]

(ii) There is a resemblance to the trimethylamine adduct[13] in that the Ga–P distance at 238.57(6) pm appears to be somewhat shorter than in the gaseous molecule, with the difference of 5.7 pm amounting to about ten standard deviations.

(iii) The P–Ga–H angle opens out appreciably from 98.4(12)° in the gaseous molecule to 106.1(6)° in the crystal. The decidedly flattened GaH_3 pyramid with H–Ga–H interbond angles of 117.9° indicated by the GED measurements thus gives place to a more sharply pitched one with H–Ga–H = 112.3(10) or 113.3(17)°.

Within the limits of uncertainty and compatibility set by the X-ray and GED experiments, these are the only structural features of $Me_3P{\cdot}GaH_3$ that vary perceptibly with the transition from the vapour to the crystal.

Table 6 Dimensions of molecules of the type $R_3E{\cdot}MY_3$ (R = organic group; E = N or P; M = B, Al, or Ga; Y = H, Me, or Cl)[a]

Compound	E–MY_3 unit			R_3E unit		Reference
	r(M–E)	r(M–Y)	Semi-vertical MY_3 angle	r(E–C)	Semi-vertical EC_3 angle	
$Me_3N{\cdot}AlH_3$(g)[b]	206.3(7)	158.5(2)	81.9(6)	148.7(2)	70.1(2)	34
$Me_3N{\cdot}GaH_3$(g)[c]	213.4(4)	151.1(13)	80.7(8)	147.6(3)	71.2(2)	13
$Me_3N{\cdot}GaH_3$(s)[d]	208.1(4)	151(6)	83(2)	147.7(4)	70.2(2)	13
$Me_3P{\cdot}GaH_3$(g)[e]	244.3(6)	159.0(11)	81.6(12)	184.0(2)	62.3(3)	This work
$Me_3P{\cdot}GaH_3$(s)[d]	238.57(6)	154(1)	73.9(6)	179.5(1)	66.3(8)	This work
$Me_3P{\cdot}BH_3$(g)[b]	190.1(7)	121.2(10)	74.9(6)	181.9(10)	66.4(4)	46
$Me_3P{\cdot}BCl_3$(s)[d]	195.7(5)	185.5(5)	72.3(2)	181.5(6)	69.2(2)	48
$Me_3P{\cdot}AlMe_3$(g)[f]	253(4)	197.3(3)	80.0(13)	182.2(3)	65.0(7)	45
$Me_3P{\cdot}GaMe_3$(g)[f]	252(2)	199.7(8)	81.6	184(1)	64.3	44
$Me_3P{\cdot}GaCl_3$(s)[d]	235.2(2)	217.1(2)	70.0(1)	179.4(9)	68.7(3)	47
$Me_3P{\cdot}GaH_2Cl$(s)[d]	238.9(15)	160 (H) 224.8(18) (Cl)	–	179.8(7)	67.0(17)	49
$Bu^t_3P{\cdot}AlH_3$(s)[d]	247.1(3)	–	–	190.1(7)	71.1(3)	12*a*
$Bu^n_3P{\cdot}GaH_3$(s)[d]	244.4(6)	–	–	190.3(20)	71.4(7)	12*a*
$Cy_3P{\cdot}AlH_3$(s)[d]	246.7(1)	160(3)	76.8(10)	184.9(3)	68.2(8)	12*b*
$Cy_3P{\cdot}GaH_3$(s)[d]	246.0(2)	148	70.7	184.2(8)	68.1(3)	12*b*

[a] Distances in pm, angles in °. [b] Microwave study (r_0 structure). [c] GED study (r_α structure). [d] X-Ray crystallographic study. [e] GED study (r_{hl} structure). [f] GED study (r_a structure).

Discussion

The present quantum chemical, GED and X-ray diffraction study is one of the few to offer a structural characterisation of an alane or gallane adduct that spans both the vapour and condensed states and includes a reasonably precise mensuration of the L–MH_3 unit (L = donor molecule; M = Al or Ga). So far as we are aware, only $Me_3N{\cdot}AlH_3$ [31,32] and $Me_3N{\cdot}GaH_3$ [13] have featured in similar studies. Included for comparison in Table 6 are selected structural data for some related complexes including variously AlH_3, GaH_3 and Me_3P as constituents.

The overall structure of the gaseous molecule is unremarkable. At 244.3(6) pm the Ga–P distance is well within the limits of 235–268 pm established for a variety of other tetracoordinated complexes of gallium(III) containing a neutral phosphine ligand, admittedly in the solid state for the most part.[5] It is thus 30.9 pm longer than the Ga–N bond in the gaseous $Me_3N{\cdot}GaH_3$ molecule, as expected on the basis of the difference in the covalent radii of P and N (35 pm).[39] Although direct comparisons are not always possible, the accumulated evidence of earlier crystallographic studies is that Ga–P distances in phosphine–gallane complexes are marginally shorter than Al–P distances in comparable alane derivatives. More significant, though, is the finding that the Al–P bond is so much longer than the Al–N one in analogous amine–alane complexes. For example, the Al–P bond in crystalline $Bu^t_3P{\cdot}AlH_3$ [12*a*] is 49.2 pm longer than the Al–N bond in $Bu^n_3N{\cdot}AlH_3$.[40] These structural details reflect the degree to which GaH_3 is better able to function as an acidic receptor to a phosphine base or, put another way, is a 'softer' acid than AlH_3.

Perhaps the most notable feature of gaseous $Me_3P{\cdot}GaH_3$ is the large semi-vertical angle of 81.6(12)° displayed by the GaH_3 fragment (to be compared with 81.0° according to *ab initio* calculations at the MP2 level with a 6-311+G(df,p) basis set). As in $Me_3N{\cdot}GaH_3$ where the same angle is 80.7(8)°,[13] therefore, the GaH_3 unit forms a very shallow pyramid not far removed from the planar skeleton of the base-free GaH_3 molecule.[41] On the evidence of both experimental and theoretical studies of complexes of the type $L{\cdot}MH_3$ formed by a Group 13 element M, the semi-vertical angle of the MH_3 component offers an index to the L⟶M binding, approaching the tetrahedral value of 70.5° when a strong covalent interaction links M and L and 90° when the interaction is only weak.[42] Hence the present results add to the collective experience of GaH_3 as a comparatively weak Lewis acid, distinctly inferior in its acceptor power to $GaCl_3$, for example.

At the same time, while coordination does not affect perceptibly the interatomic distances of the phosphine, there is a slight opening out of the semi-vertical angle of the PC_3 skeleton from 61.1(2)° for the free ligand[43] to 62.3(3)° in the complex. This is wholly in character with the normal behaviour of a phosphine ligand such as Me_3P on coordination to a main group acceptor site, M,[42] and as P⟶M charge transfer increases, so the semi-vertical angle of the PC_3 pyramid widens. Thus, with reference to other trimethylphosphine complexes, we note how the angle tracks the acceptor capacity of the Group 13 substrate in the following series: free Me_3P(g) 61.1(2)°,[43] $Me_3P{\cdot}GaMe_3$(g) 64.3°,[44] $Me_3P{\cdot}AlMe_3$(g) 65.0(7)°,[45] $Me_3P{\cdot}BH_3$(g) 66.4(4)°,[46] $Me_3P{\cdot}GaCl_3$(s) 68.7(3)°,[47] $Me_3P{\cdot}BCl_3$ 69.2(2)°.[48] How the Me_3P molecule responds structurally to coordination contrasts strikingly with the comparative insensitivity of the less polarisable Me_3N molecule.[13,42]

The $Me_3P{\cdot}GaH_3$ molecule retains its integrity on crystallisation, with no evidence of specific secondary interactions in the crystal at 150 K. The molecule may favour an eclipsed C_3PGaH_3 skeleton in these circumstances but, as our calculations suggest, a relatively trifling investment of energy is needed for intermolecular forces to overcome the natural preference of the free molecule for a staggered conformation. At the same time, crystallisation results in a shortening of the Ga–P linkage (by 5.7 pm). As in the case of $Me_3N{\cdot}GaH_3$,[13] this can be understood in terms of an increased degree of P⟶Ga charge transfer induced by the permittivity of the crystal environment, with the enhanced dipole moment serving to strengthen the intermolecular binding. Consistent with such a change is the decrease in the semi-vertical angle of the GaH_3 unit [from 81.6(12) to 73.9(6)°] and accompanying increase in the corresponding angle of the PC_3 unit [from 62.3(3) to 66.3(8)°].

For another perspective we turn to quantum chemical [MP2 calculations with a 6-311++G(d,p) basis set] estimates of the binding energy ΔE of complexes of the type $R_3E{\cdot}MH_3$ (R = H or Me; E = N or P; M = Al or Ga) as given by the energy change accompanying the dissociation reaction (1).

$$R_3E{\cdot}MH_3(g) \longrightarrow R_3E(g) + MH_3(g) \qquad (1)$$

The results of the calculations, listed in Table 7, reveal the following features of interest.

(i) The two bases NH_3 and Me_3N bind more effectively to AlH_3 than to GaH_3 with values of ΔE that differ in both cases by about 30 kJ mol^{-1}.

Table 7 Dissociation energies, ΔE, for the adducts $R_3E{\cdot}MH_3$ (R = H or Me; E = N or P; M = Al or Ga)[a]

Compound	Dissociation energy/kJ mol^{-1}
$H_3N{\cdot}AlH_3$	109.46
$H_3N{\cdot}GaH_3$	81.37
$H_3P{\cdot}AlH_3$	50.69
$H_3P{\cdot}GaH_3$	42.86
$Me_3N{\cdot}AlH_3$	129.21
$Me_3N{\cdot}GaH_3$	102.10
$Me_3P{\cdot}AlH_3$	92.98
$Me_3P{\cdot}GaH_3$	82.67

[a] MP2 calculations with a 6-311++G(d,p) basis set.

(ii) By contrast, the phosphines PH_3 and Me_3P bind more weakly to AlH_3 and GaH_3 than do NH_3 and Me_3N, with values of ΔE that differ by 8–10 kJ mol^{-1} according to whether Al or Ga is the acceptor site.

(iii) Whatever the NMR studies of benzene solutions might suggest [reaction (2)],[9]

$$Me_3N \cdot GaH_3 + Me_3P \rightleftharpoons Me_3P \cdot GaH_3 + Me_3N \quad (2)$$

$Me_3N{\cdot}GaH_3$ is more strongly bound (by about 19 kJ mol^{-1}) than is $Me_3P{\cdot}GaH_3$. This difference is not so great, however, that the markedly greater volatility of Me_3N at room temperature, compared with Me_3P, cannot introduce an entropy term sufficient to counteract the balance of binding energies, and so give an equilibrium constant near to unity for reaction (2).

Competing with complexation is the natural tendency of the free MH_3 molecule to aggregate in the condensed phase, as represented by eqn. (3).

$$MH_3(g) \longrightarrow \frac{1}{n}[MH_3]_n(c) \quad (3)$$

From no source are reliable figures available for the energetics of this process. On the basis of experimental and theoretical data,[2,5,49] however, the best (rough) estimates of ΔE for this reaction are -170 and <-50 kJ mol^{-1} for M = Al and Ga, respectively. This emphasises the fineness of the balance between complexation and dissociation to yield either the parent hydride (M = Al)[10] or its decomposition products (M = Ga).[2,14] It also highlights one of the major limitations of alane and gallane adducts as source materials for chemical vapour deposition of the metals or III–V semiconductor materials.[3–5,13]

Acknowledgements

We thank the EPSRC (i) for financial support of both the Edinburgh Electron Diffraction Service and the Oxford group, (ii) for an Advanced Research Fellowship (T. M. G.), and (iii) for a studentship (C. Y. T.).

References

1 M. J. Taylor and P. J. Brothers, in *Chemistry of Aluminium, Gallium, Indium and Thallium*, ed. A. J. Downs, Blackie, Glasgow, 1993, pp. 118–128.
2 A. J. Downs and C. R. Pulham, *Adv. Inorg. Chem.*, 1994, **41**, 171; A. J. Downs and C. R. Pulham, *Chem. Soc. Rev.*, 1994, **23**, 175.
3 M. G. Gardiner and C. L. Raston, *Coord. Chem. Rev.*, 1997, **166**, 1.
4 A. J. Downs, *Coord. Chem. Rev.*, 1999, **189**, 1.
5 S. Aldridge and A. J. Downs, *Chem. Rev.*, 2001, **101**, 3305.
6 C. Jones, *Chem. Commun.*, 2001, 2293.
7 P. Jungwirth and R. Zahradnik, *J. Mol. Struct., THEOCHEM*, 1993, **283**, 317; M. Chaillet, A. Dargelos and C. J. Marsden, *New J. Chem.*, 1994, **18**, 693; K. D. Dobbs, M. Trachtman, C. W. Bock and A. H. Cowley, *J. Phys. Chem.*, 1990, **94**, 5210.
8 K. A. Grencewicz and D. W. Ball, *J. Phys. Chem.*, 1996, **100**, 5672.
9 N. N. Greenwood, E. J. F. Ross and A. Storr, *J. Chem. Soc.*, 1965, 1400.
10 J. L. Atwood, K. W. Butz, M. G. Gardiner, G. A. Koutsantonis, C. L. Raston and K. D. Robinson, *Inorg. Chem.*, 1993, **32**, 3482.
11 J. D. Odom, K. K. Chatterjee and J. R. Durig, *J. Phys. Chem.*, 1980, **84**, 1843.
12 (*a*) F. M. Elms, M. G. Gardiner, G. A. Koutsantonis, C. L. Raston, J. L. Atwood and K. D. Robinson, *J. Organomet. Chem.*, 1993, **449**, 45; (*b*) J. L. Atwood, K. D. Robinson, F. R. Bennett, F. M. Elms, G. A. Koutsantonis, C. L. Raston and D. J. Young, *Inorg. Chem.*, 1992, **31**, 2673; F. R. Bennett, F. M. Elms, M. G. Gardiner, G. A. Koutsantonis, C. L. Raston and N. K. Roberts, *Organometallics*, 1992, **11**, 1457.
13 P. T. Brain, H. E. Brown, A. J. Downs, T. M. Greene, E. Johnsen, S. Parsons, D. W. H. Rankin, B. A. Smart and C. Y. Tang, *J. Chem. Soc., Dalton Trans.*, 1998, 3685.
14 C. R. Pulham, A. J. Downs, M. J. Goode, D. W. H. Rankin and H. E. Robertson, *J. Am. Chem. Soc.*, 1991, **113**, 5149.
15 A. J. Blake, P. T. Brain, H. McNab, J. Miller, C. A. Morrison, S. Parsons, D. W. H. Rankin, H. E. Robertson and B. A. Smart, *J. Phys. Chem.*, 1996, **100**, 12280; P. T. Brain, C. A. Morrison, S. Parsons and D. W. H. Rankin, *J. Chem. Soc., Dalton Trans.*, 1996, 4589.
16 C. A. Morrison, B. A. Smart, P. T. Brain, C. R. Pulham, D. W. H. Rankin and A. J. Downs, *J. Chem. Soc., Dalton Trans.*, 1998, 2147.
17 A. J. Downs, T. M. Greene, E. Johnsen, P. T. Brain, C. A. Morrison, S. Parsons, C. R. Pulham, D. W. H. Rankin, K. Aarset, I. M. Mills, E. M. Page and D. A. Rice, *Inorg. Chem.*, 2001, **40**, 3484.
18 P. F. Souter, D. Phil. Thesis, University of Oxford, 1995.
19 C. M. Huntley, G. S. Laurenson and D. W. H. Rankin, *J. Chem. Soc., Dalton Trans.*, 1980, 954.
20 J. R. Lewis, P. T. Brain and D. W. H. Rankin, *Spectrum*, 1997, **15**, 7.
21 S. Cradock, J. Koprowski and D. W. H. Rankin, *J. Mol. Struct.*, 1981, **77**, 113.
22 A. W. Ross, M. Fink and R. Hilderbrandt, *International Tables for Crystallography*, ed. A. J. C. Wilson, Kluwer Academic Publishers, Dordrecht, Boston and London, 1992; vol. C, p. 245.
23 G. M. Sheldrick, SADABS, University of Göttingen, Germany and Bruker AXS, Madison, WI, 2001.
24 G. M. Sheldrick, SHELXS, University of Göttingen, Germany, 1997.
25 D. J. Watkin, C. K. Prout, J. R. Carruthers, P. W. Betteridge and R. I. Cooper, CRYSTALS Issue 11, Chemical Crystallography Laboratory, Oxford, UK, 2001.
26 Gaussian 98 (Revision A.7), M. J. Frisch, G. W. Trucks, H. B. Schlegel, G. E. Scuseria, M. A. Robb, J. R. Cheeseman, V. G. Zakrzewski, J. A. Montgomery, Jr., R. E. Stratmann, J. C. Burant, S. Dapprich, J. M. Millam, A. D. Daniels, K. N. Kudin, M. C. Strain, O. Farkas, J. Tomasi, V. Barone, M. Cossi, R. Cammi, B. Mennucci, C. Pomelli, C. Adamo, S. Clifford, J. Ochterski, G. A. Petersson, P. Y. Ayala, Q. Cui, K. Morokuma, D. K. Malick, A. D. Rabuck, K. Raghavachari, J. B. Foresman, J. Cioslowski, J. V. Ortiz, A. G. Baboul, B. B. Stefanov, G. Liu, A. Liashenko, P. Piskorz, I. Komaromi, R. Gomperts, R. L. Martin, D. J. Fox, T. Keith, M. A. Al-Laham, C. Y. Peng, A. Nanayakkara, C. Gonzalez, M. Challacombe, P. M. W. Gill, B. Johnson, W. Chen, M. W. Wong, J. L. Andres, M. Head-Gordon, E. S. Replogle and J. A. Pople, Gaussian Inc., Pittsburgh, PA, 1998.
27 A. D. Becke, *J. Chem. Phys.*, 1993, **98**, 5648.
28 W. J. Hehre, R. Ditchfield and J. A. Pople, *J. Chem. Phys.*, 1972, **56**, 2257.
29 P. C. Hariharan and J. A. Pople, *Theor. Chim. Acta*, 1973, **28**, 213.
30 R. Krishnan, J. S. Binkley, R. Seeger and J. A. Pople, *J. Chem. Phys.*, 1980, **72**, 650.
31 A. D. McLean and G. S. Chandler, *J. Chem. Phys.*, 1980, **72**, 5639.
32 F. B. van Duijneveldt, J. G. C. M. van Duijneveldt-van de Rijdt and J. H. van Lenthe, *Chem. Rev.*, 1994, **94**, 1873.
33 ASYM40 version 4.1, L. Hedberg and I. M. Mills, *J. Mol. Spectrosc.*, 1998, **160**, 117.
34 H. E. Warner, Y. Wang, C. Ward, C. W. Gillies and L. Interrante, *J. Phys. Chem.*, 1994, **98**, 12215.
35 J. L. Atwood, F. R. Bennett, F. M. Elms, C. Jones, C. L. Raston and K. D. Robinson, *J. Am. Chem. Soc.*, 1991, **113**, 8183.
36 A. S. F. Boyd, G. S. Laurenson and D. W. H. Rankin, *J. Mol. Struct.*, 1981, **71**, 217.
37 See, for example, the discussion and references in B. Ma, J.-H. Lii, K. Chen and N. L. Allinger, *J. Am. Chem. Soc.*, 1997, **119**, 2570; V. A. Sipachev, *J. Mol. Struct. (THEOCHEM)*, 1985, **121**, 143; V. A. Sipachev, in *Advances in Molecular Structure Research*, eds.

I. Hargittai and M. Hargittai, JAI Press, Greenwich, 1999, vol. 5, p. 263.
38 C. Y. Tang, R. A. Coxall, A. J. Downs, T. M. Greene and S. Parsons, *J. Chem. Soc., Dalton Trans.*, 2001, 2141.
39 J. E. Huheey, E. A. Keiter and R. L. Keiter, *Inorganic Chemistry: Principles of Structure and Reactivity*, Harper Collins, New York, 4th edn., 1993, p. 292.
40 E. B. Lobkovskii and K. N. Semenenko, *Zh. Strukt. Khim.*, 1975, **16**, 150.
41 C. M. B. Marsh and H. F. Schaefer III, *J. Phys. Chem.*, 1995, **99**, 195.
42 A. Haaland, *Angew. Chem., Int. Ed. Engl.*, 1989, **28**, 992.
43 L. S. Bartell and L. O. Brockway, *J. Chem. Phys.*, 1960, **32**, 512.
44 L. M. Golubinskaya, A. A. Golubinskii, V. S. Mastryukov, L. V. Vilkov and V. I. Bregadze, *J. Organomet. Chem.*, 1976, **117**, C4.
45 A. Almenningen, L. Fernholt, A. Haaland and J. Weidlein, *J. Organomet. Chem.*, 1978, **145**, 109.
46 P. S. Bryan and R. L. Kuszkowski, *Inorg. Chem.*, 1972, **11**, 553.
47 J. C. Carter, G. Jugie, R. Enjalbert and J. Galy, *Inorg. Chem.*, 1978, **17**, 1248.
48 D. L. Black and R. C. Taylor, *Acta Crystallogr., Sect. B*, 1975, **31**, 1116.
49 C. Y. Tang, D.Phil Thesis, University of Oxford, 2002.